Synthesis, Transient Absorption, and Transient Resonance Raman Spectroscopy of Novel Electron Donor−Acceptor Complexes: [5,15-Bis[(4′-nitrophenyl)ethynyl]-10,20-diphenylporphinato]copper(II) and [5-[[4′-(Dimethylamino)phenyl]ethynyl]-15-[(4″-nitrophenyl)ethynyl]-10,20-diphenylporphinato]copper(II)

Steven M. LeCours,[†,§] Charles M. Philips,[†] Julio C. de Paula,*[,‡] and Michael J. Therien*[,†]

Contribution from the Department of Chemistry, University of Pennsylvania, Philadelphia, Pennsylvania 19104-6323, and Department of Chemistry, Haverford College, 370 Lancaster Avenue, Haverford, Pennsylvania 19041-1392

Received December 27, 1996. Revised Manuscript Received May 16, 1997[⊗]

Abstract: We report the synthesis, transient absorption, FT Raman, resonance Raman, time-resolved resonance Raman, and transient resonance Raman spectra of pseudo-D_{2h} symmetric [5,15-bis[(4′-nitrophenyl)ethynyl]-10,20-diphenylporphinato]copper(II) (**I**) and electronically asymmetric [5-[4′-(dimethylamino)phenyl]ethynyl]-15-[(4″-nitrophenyl)-ethynyl]-10,20-diphenylporphinato]copper(II) (**II**), which bears both electron-releasing and electron-withdrawing groups conjugated directly to the porphyrin periphery. The spectroscopic results suggest extensive electronic communication between the 5- and 15-arylethynyl groups and the porphyrin core. Relative to the parent compound, (tetraphenylporphinato)copper(II) (CuTPP), the arylethynyl substituents increase the lifetime of the excited trip-multiplet states. CuTPP, as well as compounds **I** and **II**, however, shows similar solvent-dependent dynamics: the trip-multiplet lifetimes are longer in a noncoordinating solvent such as benzene than in a coordinating solvent such as THF. This behavior is consistent with the existence of a quenching state whose effect is more pronounced upon coordination of solvent. The time-resolved resonance Raman spectrum of compound **II** shows features commonly associated with the relatively long-lived triplet excited states of copper(II) porphyrins. The transient resonance Raman spectrum of a short-lived excited state present in both compounds **I** and **II** is characterized by marked shifts in the nitro and porphyrin stretching frequencies relative to that observed for the ground states of both (4-nitrophenyl)-ethyne and (tetraphenylporphinato)copper(II). We interpret these results for the compounds **I** and **II** as arising from (i) a short-lived excited state present at early time that possesses enhanced porphyrin-to-nitro charge-transfer character with respect to the ground state and (ii) a longer-lived excited state deriving from this initially probed charge-transfer state that is largely porphyrin localized.

Introduction

One of the goals of the developing field of molecular electronics is the design of donor−acceptor (D−A) complexes capable of light-induced charge separation over long distances on the molecular scale.[1−3] For example, the fastest possible light-addressable electronic communication between nanoscale circuitry requires that the interconnects access very large molecular transition dipoles. As a result, ultrafast charge-transfer systems will likely figure prominently in proposed photo-driven molecular-scale rectifiers, transistors, and switches,[4] new technologies focusing on light-modulated data storage and retrieval,[5] as well as novel computing architectures and ultrasmall memory devices.[6]

Toward these ends, we have developed new porphyrin-based systems with unique photophysical properties.[7] Figure 1 shows examples of such structures and illustrates a new approach to engineering D−A complexes: pseudo-D_{2h} symmetric [5,15-bis-[(4′-nitrophenyl)ethynyl]-10,20-diphenylporphinato]copper(II) (**I**) and an electronically asymmetric version of the [5,15-bis-(arylethynyl)-10,20-diphenylporphinato]metal structural motif, [5-[[4′-(dimethylamino)phenyl]ethynyl]-15-[(4″-nitrophenyl)-ethynyl]-10,20-diphenylporphinato]copper(II) (**II**). There are three key design features in these complexes. First, the [5,15-bis(arylethynyl)-10,20-diphenylporphinato]metal core,[8] synthesized via metal-mediated cross-coupling of substituted aryl-

* To whom correspondence should be addressed.
† University of Pennsylvania.
‡ Haverford College.
§ Present address: Mobil Technology Company, Paulsboro Technology Center, Paulsboro, NJ 08066.

⊗ Abstract published in *Advance ACS Abstracts,* December 15, 1997.

(1) (a) Carter, F. L. *Molecular Electronic Devices I*; Decker: New York, 1982. (b) Carter, F. L. *Molecular Electronic Devices II*; Decker: New York, 1987.
(2) Lehn, J. M. *Angew. Chem., Int. Ed. Engl.* **1988**, *27*, 89−112.
(3) Burland, D. M.; Miller, R. D.; Walsh, C. A. *Chem. Rev.* **1994**, *94*, 31−75.
(4) (a) Aviram, A.; Ratner, M. A. *Chem. Phys. Lett.* **1974**, *29*, 277−283. (b) Miller, J. S. *Adv. Mater.* **1990**, *2*, 378−379. (c) Ebbesen, T. W. *New J. Chem.* **1991**, *15*, 191−198. (d) O'Neil, M. P.; Niemczyk, M. P.; Svec, W. A.; Gosztola, D.; Gaines, G. L., III; Wasielewski, M. R. *Science* **1992**, *257*, 63−65.
(5) (a) Emmelius, M.; Pawlowski, G.; Vollmann, H. W. *Angew. Chem., Int. Ed. Eng.* **1989**, *28*, 1445−1471. (b) Parthenopoulos, D. A.; Rentzepis, P. M. *Science* **1989**, *245*, 843−845. (c) Hunter, S.; Kiamilev, F.; Esener, S.; Parthenopoulos, D. A.; Rentzepis, P. M. *Appl. Opt.* **1990**, *29*, 2058−2066.
(6) (a) Hopfield, J. J.; Onuchic, J. N.; Beratan, D. N. *Science* **1988**, *241*, 817−820. (b) Hopfield, J. J.; Onuchic, J. N.; Beratan, D. N. *J. Phys. Chem.* **1989**, *93*, 6350−6357.
(7) (a) Lin, V. S.-Y.; DiMagno, S. G.; Therien, M. J. *Science* **1994**, *264*, 1105−1111. (b) Lin, V. S.-Y.; Therien, M. J. *Chem.-Eur. J.* **1995**, *1*, 645−651. (c) Goll, J. G.; Moore, K. T.; Ghosh, A.; Therien, M. J. *J. Am. Chem. Soc.* **1996**, *118*, 8344−8354.

S0002-7863(96)04436-8 CCC: $14.00

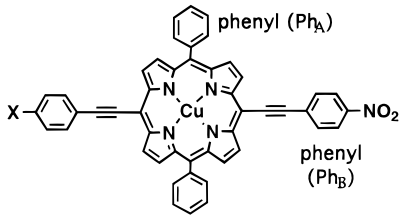

Compound **I**: x = NO_2
II: x = $N(CH_3)_2$

Figure 1. [5,15-Bis[(4′-nitrophenyl)ethynyl]-10,20-diphenylporphinato]-copper(II) (**I**) and [5-[[4′-(dimethylamino)phenyl]ethynyl]-15-[(4″-nitrophenyl)ethynyl]-10,20-diphenylporphinato]copper(II) (**II**).

ethynyl moieties to *meso*-halogenated porphyrin templates,[9] has highly polarized, singly degenerate excited states.[8,10] Second, electronic coupling between the porphyrin core and its substituents is optimized by the cylindrically π symmetric ethynyl linker. Because steric factors do not preclude a coplanar arrangement of the aromatic ring systems along the C_2 molecular axis of highest conjugation, a highly extended π system is effectively created, leading to the expectation that the arylethynyl phenyl unit and the polarizable porphyrin macrocycle will communicate electronically in both the ground and excited states. Finally, augmented electronic coupling between the (porphinato)copper(II) core and the 5- and 15-*meso* substituents is expected to enhance charge transfer to the electron-withdrawing NO_2 group.

We present transient absorption and transient resonance Raman spectra of **I** and **II**. Our results indicate that (i) there is extensive electronic coupling between the arylethynyl and porphyryl moieties, as predicted above, (ii) this electronic coupling in the short-lived, initially probed excited state exceeds that present in the ground state, (iii) this short-lived excited state with enhanced charge-transfer character evolves into a trip-multiplet state, (iv) the excited trip-multiplet states for compounds **I** and **II** have substantially longer lifetimes with respect to that reported for the parent compound, (tetraphenylporphinato)copper(II) (CuTPP), and (v) both **I** and **II** show solvent-dependent excited state dynamics similar to that observed for CuTPP: the trip-multiplet lifetimes are longer in a noncoordinating solvent such as benzene than in a coordinating solvent such as THF. We conclude that, on the basis of their photophysical properties, compounds **I** and **II** show promise as structural motifs in the development of molecular electronic devices.

Experimental Section

Transient Absorption Spectroscopy. Ground state electronic spectra were recorded on an OLIS UV/vis/near-IR spectrophotometry system that is based on the optics of a Cary 14 spectrophotometer. The transient absorption experimental setup housed at the University of Pennsylvania Regional Laser and Biotechnology Laboratory has been described previously.[11] The samples were prepared in distilled, dry solvents, and degassed by three freeze−pump−thaw cycles. Ground state electronic spectra of both compounds were recorded before and after laser irradiation to assess photostability. While compound **II** showed only slight or no photobleaching (<2%) irrespective of solvent even after prolonged laser irradiation (t > 45 min), compound **I** showed small decreases in absorbance intensity (1−2%) after 5 min and moderate photobleaching (5−6%) after 45 min of continuous irradiation.

Resonance and FT Raman Spectroscopies. All Raman spectra (FT, resonance, and time-resolved resonance) were acquired as described previously.[12,13] The ground state resonance Raman spectra were recorded with the same instrument and geometries as the transient resonance Raman spectra except that a continuous-wave Liconix 2040 HeCd laser (excitation wavelength 441.6 nm, 25 mW) was used. The FT Raman spectra were obtained with a Nicolet Raman 950 spectrometer with a Nd:YVO_4 laser (1064 nm, 300 mW) for excitation. Solvent bands were digitally subtracted.

Transient Resonance Raman Spectroscopy. One-laser transient Raman spectra were obtained with pulsed excitation at 436 nm (5 ns, 10 Hz), with instrumentation described previously.[13] High-power spectra were obtained at 16 or 28 mW while low-power spectra were obtained by placing neutral-density filters in front of the high-power beam to attenuate the power (1.2 or 2.1 mW). The low-intensity spectra seen in Figures 7B and 8B were acquired by defocusing an approximately 10 mW beam and signal-averaging the data over several hours in order to obtain transient Raman data in which ground state modes dominated the spectrum. All spectra were recorded at room temperature in the back-scattering geometry. Spectral subtractions and data handling were performed with the methodology described by de Paula *et al.*[13] to ensure data quality and reproducibility. Band maxima reported in this paper were reproducible to <2 cm^{-1} under the conditions employed. Compounds **I** and **II** were examined by FT Raman and ground state electronic absorption spectroscopy and thin-layer chromatography (TLC) before and after transient resonance Raman spectroscopy experiments were performed; in all cases, no significant decomposition was observed. While we did observe some irreversible photochemistry of compound **I** during the transient absorption measurements (see the Results), the back-scattering geometry of the Raman measurements coupled with the higher sample concentrations used in these experiments appear to have minimized the effect even in spite of the fact that photon fluxes are typically higher in Raman experiments than in absorption experiments.

Two-laser time-resolved Raman spectra were obtained with the same spectrograph and detector described previously.[13] The pump wavelength of $\lambda_{pump} = 436$ nm (tightly focused, 5 mW, 10 Hz) was generated as described above. The probe beam at $\lambda_{probe} = 532$ nm was the second harmonic of a second Continuum Surelite laser (defocused, 20 mW, 10 Hz). The beams were made to excite the same rectangular spot on the sample. Raman scattering was collected in the back-scattering geometry at room temperature. Both lasers were triggered externally by a Stanford Research Systems DG535 digital delay generator. The time delay between the pulses was $\Delta t = 10$ ns.

Electronic Structure Calculations. Frontier orbital energies for compounds **I** and **II** were determined by the ZINDO method with standard INDO-1 semiempirical parameters.[14] Molecular structure files were created in the following manner: zinc analogs of compounds **I** and **II** were first constructed with D_{2h} or C_s symmetry, respectively, in which the central zinc metal atoms were assigned a dsp^2 (square planar) geometry. For computational simplicity, ZINDO-optimized geometrical structures were obtained in which the dihedral angles of the 5- and 15-arylethynyl phenyl moieties were initially adjusted to 0° and the 10- and 20-*meso*-phenyl groups were fixed at 90° with respect to the porphyrin least-squares plane. The convergence criteria for these restricted Hartree−Fock (RHF) self-consistent field (SCF) calculations required the root mean square difference in the elements of the density matrix to be below 0.000 001 on two successive SCF cycles. Once an optimized (porphinato)zinc(II) structure was obtained, the central porphyrin zinc atom was replaced by a copper(II) center (dsp^2 hybridization; square planar geometry) and a ZINDO energy calculation was performed. Because the d^9 copper(II) electronic configuration has a ground state doublet spin multiplicity, a restricted open-shell Hartree−Fock (ROHF) SCF calculation was run (compound **I**, CI = 18;

(8) LeCours, S. M.; DiMagno, S. G.; Therien, M. J. *J. Am. Chem. Soc.* **1996**, *118*, 11854−11864.
(9) (a) DiMagno, S. G.; Lin, V. S.-Y.; Therien, M. J. *J. Am. Chem. Soc.* **1993**, *115*, 2513−2515 . (b) DiMagno, S. G.; Lin, V. S.-Y.; Therien, M. J. *J. Org. Chem.* **1993**, *58*, 5983−5993.
(10) LeCours, S. M.; Jahn, L.; Therien, M. J. Manuscript in preparation.
(11) Papp, S.; Vanderkooi, J. M.; Owen, C. S.; Holtom, G. R.; Phillips, C. M. *Biophys. J.* **1990**, *58*, 177−186.
(12) de Paula, J. C.; Walters, V. A.; Nutaitis, C.; Lind, J.; Hall, K. *J. Phys. Chem.* **1992**, *96*, 10591−10594.
(13) de Paula, J. C.; Walters, V. A.; Jackson, B. A.; Cardozo, K. *J. Phys. Chem.* **1995**, *99*, 4373−4379.
(14) ZINDO Software provided by: CAChe Scientific (Beaverton, Oregon).

compound **II**, CI = 12). The convergence criteria were identical to those used for geometry optimization. The results of these calculations were pictorially generated (tabulated) utilizing an isosurface value of 0.04.

Materials. All compounds were handled using methods and protocols described previously.[9]

(5,15-Dibromo-10,20-diphenylporphinato)zinc(II), (4-Substituted phenyl)acetylenes, and [5-[[4′-(Dimethylamino)phenyl]ethynyl]-15-[(4′′-nitrophenyl)ethynyl]-10,20-diphenylporphinato]copper(II). *p*-(Dimethylamino)phenyl)acetylene and (*p*-nitrophenyl)acetylene were synthesized similarly to literature methods.[15] The syntheses of (5,15-dibromo-10,20-diphenylporphinato)zinc(II),[9] [5,15-bis[(4′-nitrophenyl)-ethynyl]-10,20-diphenylporphinato]zinc(II),[8] and [5-[[4′-(dimethylamino)-phenyl]ethynyl]-15-[(4′′-nitrophenyl)ethynyl]-10,20-diphenylporphinato]copper(II)[16] have been previously described.

[5,15-Bis[(4′-nitrophenyl)ethynyl]-10,20-diphenylporphinato]copper(II) (I). [5,15-Bis[(4′-nitrophenyl)ethynyl]-10,20-diphenylporphinato]zinc(II)[8] was placed in a 125-mL Erlenmeyer flask and dissolved with a 1:1 mixture of THF−$CHCl_3$ (60 mL). To the green porphyrin solution was added dropwise a 2 M HCl solution diluted in 1:1 THF−2-propanol. After 5 min, the reaction mixture was poured into a 250-mL separatory funnel containing a 1 M KOH solution (30 mL). The mixture was shaken and the organic layer collected and washed once more with distilled water. The organic solvents were then removed by flash evaporation, and the crude free base porphyrin was used without further purification.

5,15-Bis[(4′-nitrophenyl)ethynyl]-10,20-diphenylporphyrin (9.3 mg, 12 mmol) was added to a 250-mL round bottom flask containing toluene (100 mL) and cupric acetate dihydrate (110 mg, 551 mmol). After being refluxed for 8 h, the reaction mixture was placed in a 250-mL separatory funnel and washed twice with 1 M ammonium hydroxide solution (30 mL) and once with water. The toluene layer was evaporated to a 15-mL total volume and chromatographed on silica gel using toluene as the eluant. A green band was collected and recrystallized to give compound **I**, isolated as a dark green solid (5.1 mg, 51%). Vis (THF): 450, 636.

Results

Ground State Electronic Spectroscopy. Compared to that of the parent compound, CuTPP, the ground state electronic spectra of complexes **I** and **II** exhibit red shifted, broader B- (also called Soret) and Q-type absorption bands at about 450 nm and 630−650 nm, respectively (Figure 2), consistent with inclusion of the arylethynyl moieties in the π frameworks of **I** and **II**. Studies of electronically symmetric [5,15-bis(arylethynyl)-10,20-diphenylporphinato]zinc(II) complexes demonstrate that a large share of the oscillator strength of both the B and Q transitions is polarized along the C_2 molecular axis of highest conjugation.[8,10]

Transient Absorption Spectroscopy. Figures 3 and 4 show the transient absorption spectra at various time delays for compounds **II** and **I**, respectively, in THF and benzene. Table 1 lists the excited state lifetimes for **I** and **II** and compares them to data for the CuTPP parent compound.

The spectra are dominated by a transient bleach nearly coincident with the location of the ground state Soret band (∼450 nm) and by transient absorption bands on both sides of this bleach. The spectra recorded in THF and benzene for **II** (parts A and B, respectively, of Figure 3) are characterized by symmetrical recovery of all transient features and by two solvent-independent isosbestic points at 396 and 483 nm. The Soret bleach recovers and the transient absorption decays with indistinguishable, monoexponential kinetics.

Unlike the transient absorption spectra for compound **II**, those

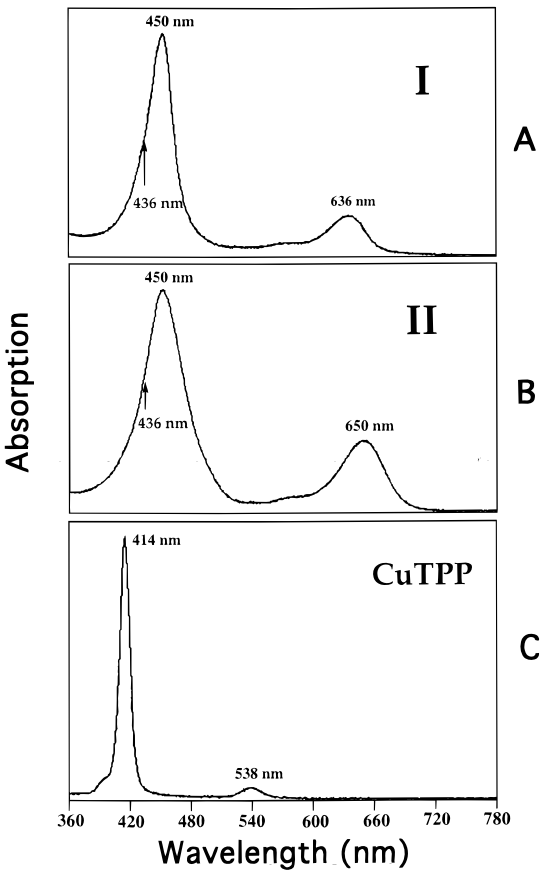

Figure 2. Electronic spectra of (porphinato)copper complexes recorded in THF: (A) compound **I**; (B) compound **II**; (C) CuTPP.

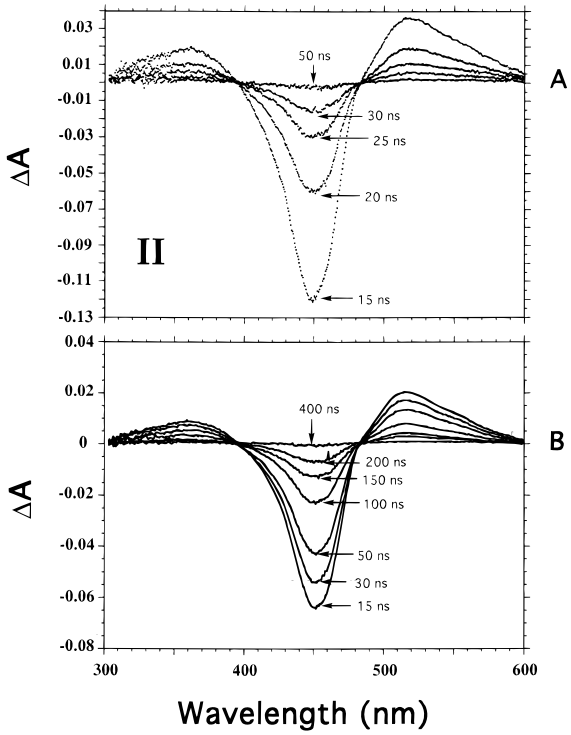

Figure 3. Transient absorption spectrum of compound **II** recorded at various time delays: (A) THF, 15 → 50 ns; (B) benzene, 15 → 400 ns.

(15) (a) Eastmond, R.; Walton, D. R. M. *Tetrahedron* **1972**, *28*, 4591−4599. (b) Westmijze, H.; Vermeer, P. *Synthesis* **1979**, 390−392. (c) Takahashi, S.; Kuroyama, Y.; Sonogashira, K.; Hagihara, N. *Synthesis* **1980**, 627−630. (d) Mesnard, D.; Bernadou, F.; Miginiac, L. *J. Chem Res. (S)* **1981**, 270−271. (e) Zhang, Y.; Wen, J. *Synthesis* **1990**, 727−728. (f) Park, K. M.; Schuster, G. B. *J. Org. Chem.* **1992**, *57*, 2502−2504.

(16) (a) LeCours, S. M.; Guan, H.-W.; DiMagno, S. G.; Wang, C. H.; Therien, M. J. *J. Am. Chem. Soc.* **1996**, *118*, 1497−1503. (b) Priyadarshy, S.; Therien, M. J.; Beratan, D. N. *J. Am. Chem. Soc.* **1996**, *118*, 1504−1510.

Table 1. Excited State Triplet Lifetime Data of **I** and **II** Obtained from Transient Absorption Experiments[a]

	triplet state lifetime (ns)				
	compound **I**[b]		compound **II**[b]		
solvent	absorption decay	Soret recovery	absorption decay	Soret recovery	CuTPP[c]
benzene	77 ± 6 (75%) $(7 \pm 2) \times 10^2$ (25%)	45 ± 2	92 ± 3[d]	82.3 ± 0.9	35
THF	5.3 ± 0.6 (97%) $(6 \pm 1) \times 10^2$ (3%)	5.8 ± 0.4[e]	8.3 ± 0.5	7.2 ± 0.1	0.035[f]

[a] Experimental conditions: pump wavelength 630 nm, power 150 mW, $T = 25$ °C. All the time-resolved data could be fit as either single exponential (compound **I**) or biexponential (compound **II**) decays over a minimum of 5 lifetimes of the fast component. Analyses of the goodness of the data fit corresponded to minimum values of χ^2 of 0.995 and 0.9994 for the biexponential and single exponential decay processes, respectively. Wavelengths chosen for monitoring transient absorption and bleaching were those that corresponded to the maximal extinction coefficient. [b] Rate constants reported ± their standard errors. The percentage of respective components for the biexponential decay processes is given in parentheses. [c] See ref 28a. [d] The data are better fit to a biexponential decay ($\chi^2 = 0.9993$) with $\tau_1 = 79 \pm 7$ ns (93%) and $\tau_2 = 610 \pm 1100$ ns (7%). [e] The data fit a single exponential decay after utilizing a nonzero baseline correction. [f] In THF, CuTPP decays with two time constants, 35 and 190 ps; the former time constant has been assigned to the decay of the triplet state while the nature of the state giving rise to the latter decay has not been identified.[25,28]

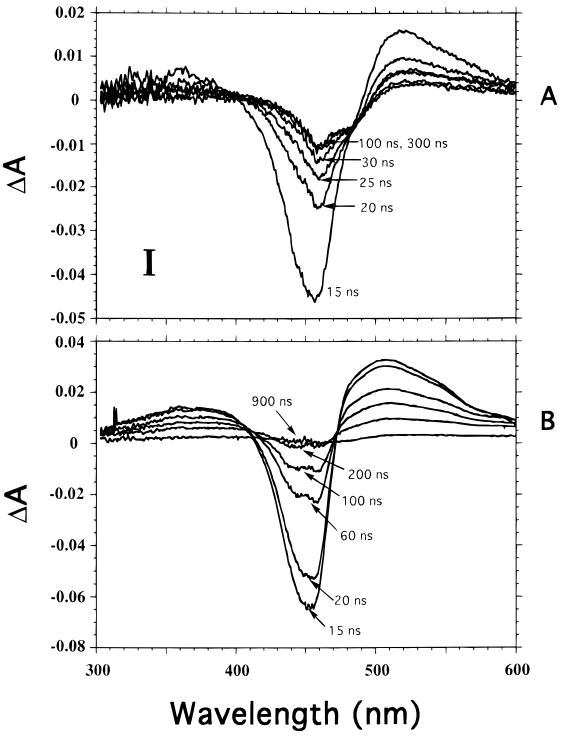

Figure 4. Transient absorption spectrum of compound **I** recorded at various time delays: (A) THF, 15 → 300 ns; (B) benzene, 15 → 900 ns.

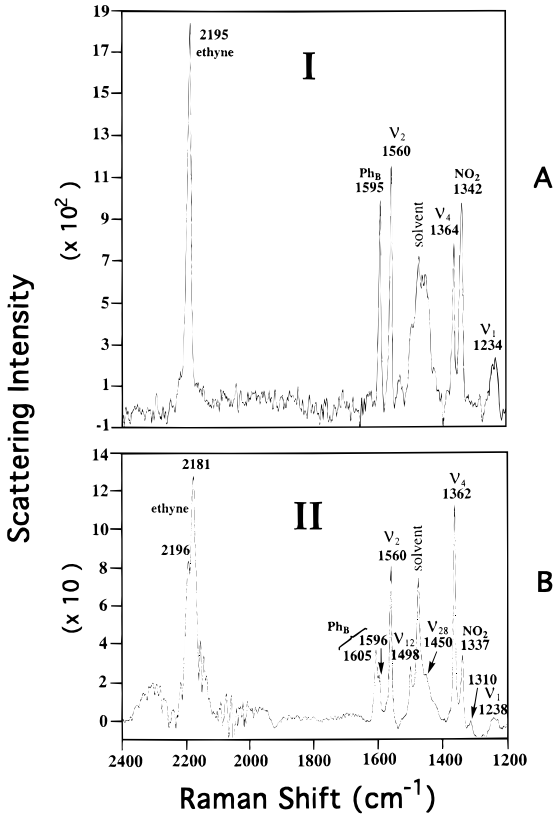

Figure 5. FT Raman spectra of (porphinato)copper complexes **I** and **II** recorded in THF solution. (A) compound **I**; (B) compound **II** (excitation wavelength 1064 nm, laser power 300 mW, $T = 25$ °C).

obtained for **I** (Figure 4) are more complex and lack well-defined isosbestic points. Moreover, compound **I**'s absorption decay kinetics are not single exponential in nature. With increasing time, the Soret bleach feature observed in benzene (Figure 4B) appears to red shift by 3 nm, flatten, and eventually split. The Soret bleach recovery ($\lambda = 455.6$ nm) for compound **I** in benzene is monoexponential, but its lifetime (44.7 ± 2.0 ns) differs from that of the fast component of the biexponential absorption decay (76.7 ± 6.3 ns) evaluated at $\lambda = 508.1$ nm. In THF (Figure 4A), the fast components of the absorption decay (5.26 ± 0.56 ns) and the Soret bleach recovery (5.82 ± 0.39 ns) are indistinguishable. However, the ground state does not recover completely even after $t > 1$ μs. Also, other spectral features appear in the 470−490 nm region of the spectrum over the 100−300 ns time domain. The complex nature of compound **I**'s transient absorption spectra suggests the irreversible formation of a photoproduct and is consistent with the partial photobleaching of **I** that occurs over the course of the transient absorption study (see the Experimental Section).

FT and Resonance Raman Spectroscopy. Figure 5 shows the FT Raman spectra of compounds **I** and **II** ($\lambda_{ex} = 1064$ nm) while parts A and B of Figure 6 display their respective resonance Raman spectra ($\lambda_{ex} = 441.6$ nm). Despite key differences in electronic and geometric structure between the [5,15-(arylethynyl)porphinato]copper(II) complexes (compounds **I** and **II**) and CuTPP, a number of striking similarities exist in their ground state FT Raman, resonance Raman, and transient Raman spectra (*vide infra*). These spectral correspondences have allowed us to assign *qualitatively* the mode compositions for these novel chromophores in lieu of performing a normal coordinate analysis.

The bands around 1600 cm^{-1} (phenyl stretch), 1560 cm^{-1} (ν_2; $C_\beta C_\beta$), 1364 cm^{-1} (ν_4; $C_\alpha N$, $C_\alpha C_\beta$), and 1230−1240 cm^{-1} (ν_1; $C_{meso}CPh$)[17] are assigned readily by analogy with the vibrational spectrum of CuTPP. Primarily due to their frequencies, two other nonporphyrinic peaks can also be assigned: the

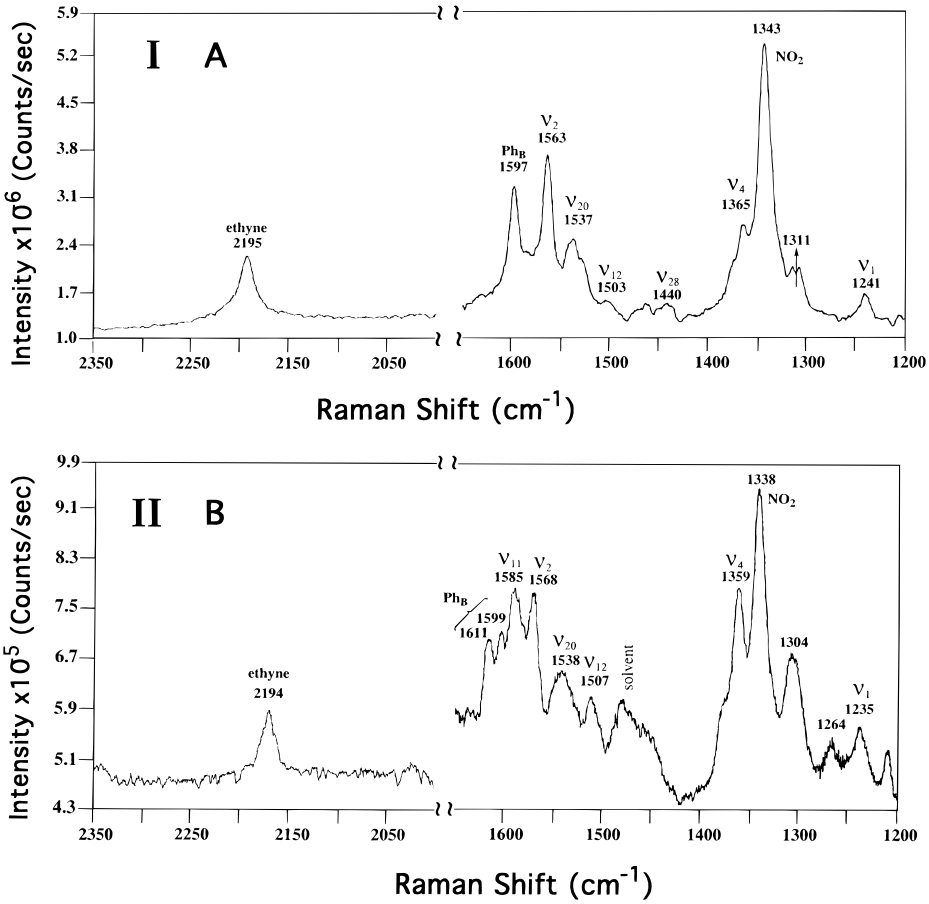

Figure 6. Resonance Raman spectra of the ethynyl and aromatic/porphyrin regions for compounds **I** and **II** recorded in THF solution: (A) compound **I**; (B) compound **II** (excitation wavelength 441.6 nm, laser power 25 mW, $T = 25$ °C).

ethynyl stretch at around 2195 cm^{-1} and the nitro stretch[18] at 1337−1343 cm^{-1}.

Many of the remaining bands in Figures 5 and 6 are not observed in the Soret-excited resonance Raman spectra of CuTPP.[19] As expected for symmetries lower than D_{4h}, many modes gain considerable intensity in compounds **I** and **II**, giving rise to more complicated spectra. On the basis of the normal coordinate analyses for CuTPP by Czernuszewicz et al.[20] and Atamian et al.,[19] we tentatively assign the bands at 1498−1507 and 1537−1538 to ν_{12} ($C_\beta C_\beta$) and ν_{20} ($C_\alpha C_{meso}$), respectively.

The main difference between the vibrational spectra of compounds **I** and **II** is that the resonance Raman spectrum of the latter has two additional peaks at 1611 and 1585 cm^{-1}. The 1611 cm^{-1} band clearly derives from the phenyl C−C stretch of the (dimethylamino)phenyl moiety (Figure 6B).[21] The 1585 cm^{-1} band probably arises from ν_{11} ($C_\alpha C_{meso}$).[19,20]

Transient Resonance Raman Spectroscopy of Compound I. Figure 7 shows the transient resonance Raman spectra for compound **I** in the aromatic/porphyrin region, obtained with 436 nm excitation (pulse width 5 ns; repetition rate 10 Hz). With the exception of frequency shifts of several vibrational bands, the spectrum of Figure 7A, obtained with high laser power, has many features in common with the Soret-excited resonance Raman spectrum of the ground state (Figure 6A). These data are consistent with the spectrum of a single state at high laser powers; this situation is somewhat unique in transient Raman spectra of metalloporphyrins, where typically the high-power spectrum shows distinct contributions from both the ground state and one or more excited states (see de Paula et al.[13] and references cited therein). It was necessary to defocus the laser pulse substantially in order to obtain the spectrum in Figure 7B, which resembles the FT Raman spectrum of compound **I** (Figure 5A). These observations indicate that the high-power spectrum of Figure 7A arises from an excited state of compound **I**.

The minor differences between the resonance Raman spectrum of Figure 6A and the transient resonance Raman spectrum of Figure 7B are probably due to one or more of three effects. First, the spectrum in Figure 7B has a low signal-to-noise ratio, which makes the determination of peak frequencies difficult. Second, the spectra in Figures 6A and 7B were obtained at different excitation wavelengths (441.6 in Figure 6A vs 436 nm in Figure 7B). It is likely that the Soret band of compound **I** (Figure 2) is inhomogeneously broadened due to (i) the

(17) Note: this peak has been labeled as both a ν_1 ($C_{meso}C_{phenyl}$) stretch[13,20] and the C mode;[19] we have elected to use the ν_1 convention. Our choice of assignment is partly based on the behavior of this mode upon formation of excited states (*vide infra*). In CuTPP, the ν_1 mode has a modestly small downshift of 2−4 cm^{-1} upon photoexcitation. Two other modes we considered as plausible alternatives to the ν_1 assignment for the 1228 cm^{-1} band were ν_{22} ($C_\alpha N$) and ν_{31} ($C_\beta H$ in-plane deformation). While the ν_{22} mode would be expected to downshift, the ν_{31} mode would be expected to be relatively insensitive to photoexcitation. The ν_{31} mode has b_{2g} symmetry in both D_{4h} and D_{2h} point groups and so would be expected to be Raman active. The ν_{22} mode, though formally Raman inactive (a_{2g} symmetry) in the D_{4h} point group, becomes the Raman allowed (b_{1g}) in D_{2h} symmetry porphyrins. On the basis of this reasoning, we suggest that the 1228 cm^{-1} band arises from either ν_1 or ν_{22}. Regardless, whether this mode is ν_1 or in fact ν_{22} does not impact our general analysis of the transient Raman spectrum of compound **I**.

(18) Akins, D. L.; Guo, C.; Zhu, H.-R. *J. Phys. Chem.* **1993**, *97*, 3974−3977.

(19) Atamian, M.; Donohoe, R. J.; Lindsey, J. S.; Bocian, D. F. *J. Phys. Chem.* **1989**, *93*, 2236−2243.

(20) Czernuszewicz, R. S.; Macor, K. A.; Li, X.-Y.; Kincaid, J. R.; Spiro, T. G. *J. Am. Chem. Soc.* **1989**, *111*, 3860−3869.

(21) LeCours, S. M.; de Paula, J. C.; Therien, M. J. Unpublished results.

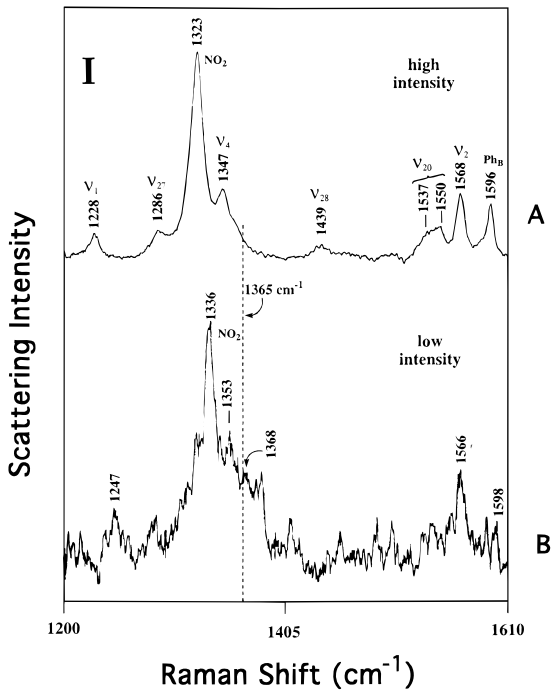

Figure 7. Transient resonance Raman spectra of the aromatic/porphyrin region of compound **I** in THF obtained with pulsed excitation at 436 nm: (A) high-intensity spectrum (power 28 mW); (B) low-intensity spectrum (laser power $\ll$ 1 mW).

disparity in oscillator strength between the extensively split *x*- and *y*-polarized transitions, (ii) the coupling of other electronic (e.g., CT) states to the normally porphyrin-localized S_2 state, (iii) spectral contributions from ground state conformations that differ with respect to the torsional angle between the arylethynyl phenyl ring and the porphyrin macrocycle, and (iv) vibronic coupling.[8,16] Such spectral complexity will likely result in the observation of vibrational signatures in the Raman experiment that are strongly dependent upon the excitation wavelength within the Soret envelope.[22] Finally, Figure 7B may contain a contribution from the excited state that gives rise to the spectrum in Figure 7A. We justify this conclusion with the observation that the spectrum in Figure 7B has a broad feature in the 1300−1385 cm^{-1} range, whereas the excited state (Figure 7A) and pure ground state spectra (Figures 5A and 6A) show only two major peaks in the same region. For these reasons, we will (i) interpret only the most intense bands in Raman spectra obtained under low-power pulsed excitation and (ii) use only data obtained at 436 nm in the interpretation of one-laser transient Raman spectra.

The low- and high-power transient Raman spectra of the ethynyl stretching frequency region of compound **I** (data not shown)[23] show that the ethynyl stretch occurs at the same frequency (2195 cm^{-1}) as it does in both the FT Raman (Figure 5A) and ground state resonance Raman (Figure 6A) spectra. Although the scaled difference spectrum for the porphyrin/aromatic region of compound **I** shows no unusual spectral features (data not shown), the analogous scaled difference spectrum in the ethynyl region[23] shows a trough at the peak of the ethynyl stretching frequency and two peaks symmetrically disposed around the trough. These data suggest that the ethynyl stretching band becomes slightly broader at high laser powers. Performing a multipoint fit to force a flat baseline for **I**'s low- and high-power transient Raman spectra and taking a scaled difference still evinces a broadened ethynyl mode at high laser power.[23] While power broadening is generally thought to arise from systems with either unrelaxed low-frequency inner sphere or solvent vibrations, or nonlinear resonance processes,[24] given the time scale of the transient experiment and the modestly-low-power densities employed in this study, it is unlikely that in this instance power broadening derives from unrelaxed molecular vibrations. On the other hand, nonlinear resonance scattering occurs typically at higher powers than used in this study. For example, the resonance Raman spectrum of β-carotene in isopentane exhibits nonlinear resonance scattering at power levels approaching 1×10^9 W/cm^2,[24b] whereas the peak power level in our experiments was 2×10^7 W/cm^2. Although it may be attractive to hypothesize that such an effect may be in accord with the established nonlinear optical properties of this class of chromophores,[16] because the extent of broadening of the ethynyl band is minor and its mechanism unclear from these experiments, these data will not be analyzed further in the Discussion. While we note that this will not impact our interpretation of the excited state dynamics of compound **I** (*vide infra*), we provide below justification for the apparent lack of a frequency shift in this band upon electronic excitation.

Transient Resonance Raman Spectra of Compound II. The low- and high-power transient resonance Raman spectra for compound **II** are shown in Figure 8. In spite of the lower symmetry of compound **II** (C_s), its transient resonance Raman spectra are very similar to those observed for compound **I**. However, three differences observed in the high-intensity spectrum are worthy of mention (Figure 8A). First, the additional feature at 1607 cm^{-1} observed in the high-intensity spectrum is related to the phenyl C−C stretch of the (dimethylamino)phenyl moiety (*vide supra*). Second, the band at 1450 cm^{-1} in Figure 8A has little or no intensity in either the ground state resonance Raman or low-laser-power transient resonance Raman spectrum, but possesses moderately high intensity in the high-power spectrum. Finally, we tentatively assign the band at 1509 cm^{-1} to the ν_{12} ($C_\beta C_\beta$) mode, which has been identified in the resonance Raman spectrum of $CuTPP^+$ (*vide infra*).[20]

The scaled transient Raman difference spectrum for the ethynyl region of compound **II** (data not shown)[23] possesses power-broadened features similar to those observed for compound **I**. Also as observed for compound **I**, the ethynyl stretching band does not shift upon electronic excitation.

Time-Resolved Resonance Raman Spectrum of Compound II. We were not able to observe reproducible features

(22) The discrepancies between data at 441.6 and 436 nm suggest complex excitation profile dependence for these modes, similar to what has been observed previously for (octaethylporphinato)nickel(II) (NiOEP) (Alden, R. G.; Crawford, B. A.; Doolen, R.; Ondrias, M. R.; Shelnutt, J. A. *J. Am. Chem. Soc.* **1989**, *111*, 2070−2072). The excitation profile for a number of modes in NiOEP was consistent with the existence of multiple conformational forms in solution that differed in their degree of porphyrin ring ruffling. Likewise, our data on compound **I** may be explained by the existence of a distribution of macrocycle conformations in solution. For example, conformers of compound **I** may exist in solution that differ with respect to their arylethynyl phenyl-to-porphyrin dihedral angles. The ambient temperature electronic spectrum of **I** (Figure 2) shows that the B band region is broader than that observed for CuTPP; while this effect likely derives primarily from the extensive splitting between the B_x and B_y states (see refs 8 and 16b), conformational heterogeneity would influence the degree of absorption band broadening as well. Consistent with this, it is important to note that the nitro band in the FT Raman experiment is approximately twice as broad as comparably intense peaks. We conclude that changing the excitation wavelength from 441.6 (Figure 6A) to 436 nm (Figure 7B) in the resonance Raman experiments likely selects populations of chromophores that are not structurally isomorphous and thus produce similar but nonsuperimposible spectra. This is congruent with the low-intensity transient resonance Raman spectrum of Figure 7B which exhibits a large number of overlapping bands.

(23) These data are available as Supporting Information.

(24) (a) Carroll, P. J.; Brus, L. E. *J. Am. Chem. Soc.* **1987**, *109*, 7613−7616. (b) Carroll, P. J.; Brus, L. E. *J. Chem. Phys.* **1987**, *86*, 6584−6590. (c) Dick, B.; Hochstrasser, R. M. *J. Chem. Phys.* **1984**, *81*, 2897−2906.

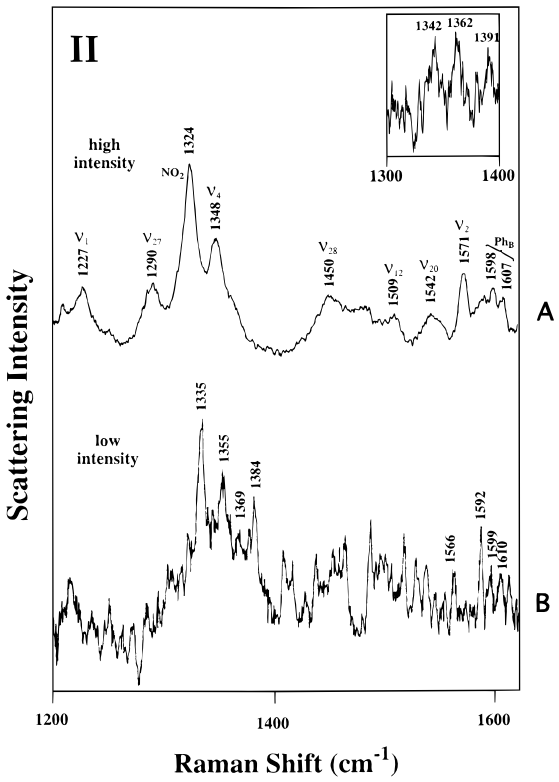

Figure 8. Transient resonance Raman spectra of the aromatic/porphyrin region of compound **II** in THF obtained with pulsed excitation at 436 nm: (A) high-intensity spectrum (power 16 mW); (B) low-power spectrum (laser power $\ll$ 1 mW). Inset: Time-resolved resonance Raman spectrum of compound **II** in piperidine ($\lambda_{pump} = 436$ nm, $\lambda_{probe} = 532$ nm, and $\Delta t = 10$ ns).

in the two-laser time-resolved resonance Raman spectrum of compound **I**, possibly due to its photoinstability (*vide supra*). While the time-resolved Raman spectra of compound **II** generally exhibited low signal-to-noise ratios, it should be noted that (i) two-laser nanosecond time-resolved resonance Raman spectra of (porphinato)copper(II) complexes are notoriously weak and (ii) the data obtained in our experiments is of quality comparable to that of published benchmark spectra for such species.[25] We observe two bands at 1342 and 1362 cm^{-1} when conditions are optimized for probing the species with a transient absorption feature at 520−530 nm ($\lambda_{pump} = 436$ nm, $\lambda_{probe} = 532$ nm, and $\Delta t = 10$ ns, inset of Figure 8).

Electronic Structure of Compounds I and II. In order to provide a framework in which to rationalize the results of our spectroscopic investigations, we performed electronic structure calculations (ZINDO; see the Experimental Section).[14] Figures 9 and 10 display the frontier orbitals (FOs) of compounds **I** and **II**, respectively, along with their calculated relative energies and symmetries.

Both Figures 9 and 10 suggest that, in the region of the porphine macrocycle, the HOMO − 1, HOMO − 2, LUMO, and LUMO + 1 are related to the a_{2u}, a_{1u}, and doubly degenerate e_g FOs of square-planar porphyrins.[26] Unlike CuTPP, whose low-energy electronic states may be explained by four porphyrin-based FOs, compounds **I** and **II** have a fifth orbital, the LUMO + 2, which is nearly identical in energy with respect to the e_g-derived LUMO + 1, where the majority of the electron

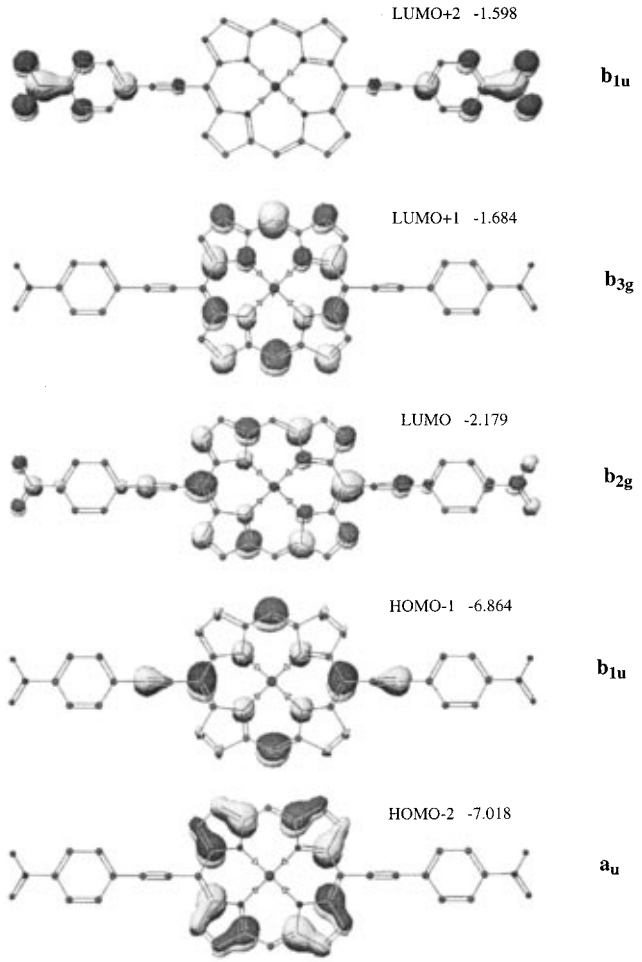

Figure 9. Frontier molecular orbitals for compound **I**. Electron density localized on the 10- and 20-*meso*-phenyl moieties is not shown. Orbital symmetries and the calculated energies are noted on the right. The half-filled HOMO, which is largely metal $d_{x^2-y^2}$ in character, is not depicted. This orbital is orthogonal to the porphyrin, ethyne, and (arylethynyl)-phenyl π-symmetry orbitals, and hence does not play a significant role in the analysis of the data reported herein.

density resides in one or both of the aryl moieties linked to the macrocycle via the ethynyl group. Our results indicate the following.

(i) The HOMO − 1 and HOMO − 2 are very close in energy.[8] This is due to the electron-withdrawing effect of the nitrophenylethynyl moiety, which stabilizes the HOMO − 1 with respect to the HOMO − 2.[8] In CuTPP the separation between the highest filled a_{2u} and a_{1u} orbitals is large enough to result in low-energy excited triplet states that are due to the $(a_{2u}e_g)$ configuration.[25,27−29] By contrast, we cannot be certain if, for example, the first excited triplet state of compound **I** will be formed by removal of the a_u (a_{1u} in D_{4h} symmetry) or b_{1u}

(25) Jeoung, S. C.; Kim, D.; Cho, D. W.; Yoon, M. *J. Phys. Chem.* **1995**, *99*, 5826−5833.
(26) Gouterman, M. In *The Porphyrins*; Dolphin, D., Ed.; Academic Press: London, 1978; Vol. III, pp 1−165.
(27) (a) Antipas, A.; Dolphin, D.; Gouterman, M.; Johnson, E. C. *J. Am. Chem. Soc.* **1978**, *100*, 7705−7709. (b) Spellane, P. J.; Gouterman, M.; Antipas, A.; Kim, S.; Liu, Y. C. *Inorg. Chem.* **1980**, *19*, 386−391. (c) Kim, D.; Holten, D.; Gouterman, M. *J. Am. Chem. Soc.* **1984**, *106*, 2793−2798. (d) Asano, M.; Kaizu, Y.; Kobayashi, H. *J. Chem. Phys.* **1988**, *89*, 6567−6576. (e) Yan, X.; Holten, D. *J. Phys. Chem.* **1988**, *92*, 5982−5986. (f) Rodriguez, J.; Kirmaier, C.; Holten, D. *J. Am. Chem. Soc.* **1989**, *111*, 6500−6506. (g) Asano-Someda, M.; Kaizu, Y. *J. Photochem. Photobiol. A* **1995**, *87*, 23−29. (h) Liu, F.; Cunningham, K. L.; Uphues, W.; Fink, G. W.; Schmolt, J.; McMillin, D. R. *Inorg. Chem.* **1995**, *34*, 2015−2018. (i) Cunningham, K. L., McNett, K. M.; Pierce, R. A., Davis, K. A.; Harris, H. H.; Falck, D. M.; McMillin, D. R. *Inorg. Chem.* **1997**, *36*, 608−613.
(28) (a) Kruglik, S. G., Apanasevich, P. A., Chirvony, V. S., Kvach, V. V. and Orlovich, V. A. *J. Phys. Chem.* **1995**, *99*, 2978−2995. (b) Asano-Someda, M.; Sato, S.; Aoyagi, K.; Kitagawa, T. *J. Phys. Chem.* **1995**, *99*, 13800−13807.

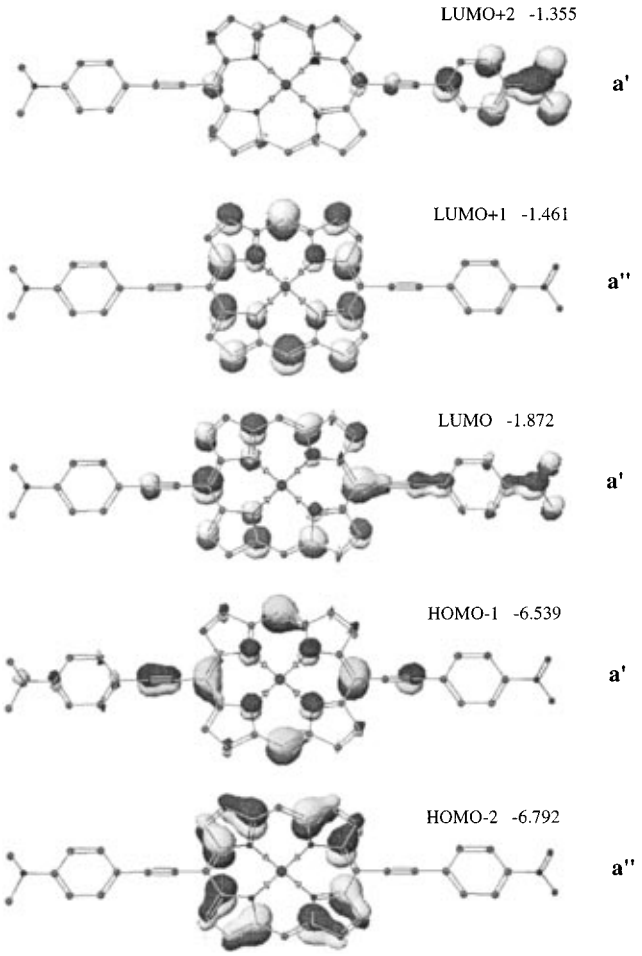

Figure 10. Frontier molecular orbitals for compound **II**. Electron density localized on the 10- and 20-*meso*-phenyl moieties is not shown. Orbital symmetries and the calculated energies are noted on the right. The half-filled HOMO, which is largely metal $d_{x^2-y^2}$ in character, is not depicted.

(a_{2u} in D_{4h} symmetry) orbital (see Figure 9). We must rely on spectroscopic evidence for such an assignment.

(ii) The LUMO and LUMO + 2 have considerable electron density at the nitro moiety; for this reason, we predict that some of the low-energy excited states have porphyrin-to-nitro charge-transfer (CT) character.

(iii) The LUMO + 1 has negligible electron density in the arylethynyl region; thus, we predict that electron promotion from either the HOMO − 2 or HOMO − 1 to the LUMO + 1 results in excited states that are localized largely within the porphyrin macrocycle.

Discussion

Electronic Coupling in Arylethynyl-Substituted Porphyrins. Our Raman spectral data (Figures 5 and 6) and electronic structure calculations (Figures 9 and 10) provide evidence for electronic coupling between the arylethynyl and (porphinato)-copper(II) moieties in the ground state of compounds **I** and **II**. The HOMO − 1 orbitals of compounds **I** and **II** indicate delocalization of electron density between the porphyrin macrocycle and the ethynyl groups. This conclusion is supported by the observation that the ethynyl stretches in compounds **I** and **II** are downshifted 25−40 cm^{-1} relative to the ethynyl frequencies typically observed in the Raman spectra of simple diarylacetylenes.[30] Ground state electronic coupling is less strong between the central (porphinato)copper(II) unit and the nitro substituent of the arylethynyl phenyl ring: the HOMO − 1 and HOMO − 2 do not exhibit appreciable electron density at the nitro group, and consequently, the frequency of the nitro band in both **I** and **II** is downshifted by only 5−10 cm^{-1} with respect to that observed in the FT Raman spectrum of (4-nitrophenyl)acetylene (1347 cm^{-1}; data not shown).

Our data also suggest that electronic coupling between the (porphinato)copper(II) core and the arylethynyl moieties is different in the ground and excited singlet states. Table 2 shows that the relative degree of enhancement of the Raman modes in compounds **I** and **II** changes upon electronic excitation in the Soret band. The nitro band is more intense than the ethynyl, ν_2 ($C_\beta C_\beta$), or ν_4 ($C_\alpha N$, $C_\beta C_\beta$) band in the resonance Raman spectrum, but is generally weaker than all of these modes in the FT Raman spectrum. Furthermore, the ethynyl stretching mode is weaker than the porphyrin bands in the resonance Raman spectrum, but stronger than the porphyrin bands in the FT Raman spectrum.

The data suggest that electronic excitation in the Soret band results in a substantial redistribution of electron density; clearly the nitro group is more strongly coupled to the porphyrin in the initially-prepared singlet excited state with respect to the ground state. By the same token, it appears that the ethynyl group is not coupled more strongly in the singlet state(s) accessible through Soret excitation than in the ground state. These observations are consistent with our electronic structure calculations, which show a significant increase in electron density at the nitro group in the LUMO and LUMO + 2, but predict less pronounced changes in electron density at the ethynyl group when the LUMOs are populated at the expense of the HOMOs.

Dynamics of Excited States Observed by Transient Absorption Spectroscopy. We discuss our data on compounds **I** and **II** in the context of theoretical and spectroscopic studies performed on their parent compound, CuTPP.[13,25,27−29] In summary, it is known that (i) efficient intersystem crossing induced by the paramagnetic d^9 Cu(II) center shortens the sing-doublet excited state lifetime to <350 fs, (ii) the initial sing-doublet excited state decays to lower energy trip-doublet (^{2}T) and trip-quartet (^{4}T) states, whose luminescence properties are both solvent and temperature dependent, (iii) the interaction between the half-filled $d_{x^2-y^2}$ metal orbital and the empty porphyrin e_g* orbitals results in a metal-to-ring (ligand) (d, π*) charge-transfer (MLCT) state, (iv) promotion of an electron from the porphyrin-centered a_{2u} orbital to the singly occupied copper $d_{x^2-y^2}$ defines a ring-to-metal (π, d) LMCT state, and (v) a d_{z^2}-to-$d_{x^2-y^2}$ (d, d) excited state can have energies similar to those of the (π, π*) and CT states.

Two models have been proposed to explain the dynamics of the ^{2}T−^{4}T manifold. On the basis of the decrease of the trip-multiplet lifetime in the presence of coordinating solvents, Kim et al.[27c] proposed that coordination lowers the energy of an excited state that quenches the ^{2}T−^{4}T manifold. Indeed, transient resonance Raman spectroscopy has shown that coordination of THF or piperidine results in the formation of an excited state that has spectral features characteristic of either a CT state[13,25] or a (d, d) state.[28a] However, Asano-Someda and Kaizu[27g] and Cunningham et al.[27i] explain modulations in the

(29) (a) Zerner, M.; Gouterman, M. *Theor. Chim. Acta (Berlin)* **1966**, *4*, 44−63. (b) Roos, B.; Sundbom, M. *J. Mol. Spectrosc.* **1970**, *36*, 8−25. (c) Case, D. A.; Karplus, M. *J. Am. Chem. Soc.* **1977**, *99*, 6182−6194. (d) Shelnutt, J. A.; Straub, K. D.; Rentzepis, P. M.; Gouterman, M.; Davidson, E. R. *Biochemistry* **1984**, *23*, 3946−3954. (e) Stavrev, K.; Zerner, M. C. *Chem. Phys. Lett.* **1995**, *233*, 179−184.

(30) In *Raman/Infrared Atlas of Organic Compounds*, 2nd ed.; Schrader, B., Ed.; VCH Publishers: New York, 1989.

Table 2. Relative Degree of Vibrational Mode Enhancements Observed for Compounds **I** and **II** in the FT and Resonance Raman Spectra[a]

		ratio of intensities							
compound	experiment	ν_2/ν_4	NO_2/ν_2	NO_2/ν_4	NO_2/ethyne	ν_2/ethyne	ethyne/ν_4	ν_2/Ph_B	Ph_B/ν_4
I	resonance Raman	1.79	1.72	3.12	3.12	1.79	1.00	1.25	1.44
I	FT Raman	1.48	0.83	1.22	0.52	0.63	2.34	1.20	1.24
II	resonance Raman	0.77	2.63	2.00	3.03	1.16	0.67	2.08	0.37
II	FT Raman	0.72	0.41	0.29	0.26	0.64	1.12	2.22	0.32

[a] Mode compositions are described in the text and listed in Table 3; Ph_B refers to the arylethynyl phenyl ring (see Figure 1).

excited state lifetime of CuTPP by invoking a vibronic interaction that broadens the excited state potential energy surface and enhances radiationless decay processes. Presumably, coordination of a solvent molecule to either the ground state (as in the case of piperidine) or the excited state (as in the case of THF) promotes the vibronic interaction through a doming distortion that pulls the Cu^{2+} ion out of the porphine plane.[27i]

The transient absorption spectra of compounds **I** and **II** (Figures 3 and 4) show features that are qualitatively similar to those observed in triplet−triplet absorption spectra of (porphinato)copper(II) complexes.[27c,e,f,28a] Hence, we assign the transient absorption features in the 300−400 and 500−550 nm regions to electronic excitation of the $^2T-{}^4T$ states of compounds **I** and **II**.

The triplet state lifetimes in compounds **I** and **II** are approximately 80 ns in noncoordinating benzene and are longer by a factor of 2−3 relative to the triplet state lifetime of CuTPP under similar experimental conditions.[27c,e,f] These data alone do not allow us to attribute the increase in lifetime to a specific substituent effect because McMillin and co-workers[27h,i] have shown that the triplet state lifetimes of arene-ring-substituted CuTPPs do not vary systematically with the electronic properties of the phenyl substituent. In order to interpret the dynamics of the $^2T-{}^4T$ manifold in our donor−acceptor complexes, we examined the influence of solvent on the transient absorption spectra. As noted in Table 1, the triplet lifetimes for **I** and **II** in coordinating THF are shorter than those that are observed in benzene; it is important to recognize, however, that the triplet lifetimes for **I** and **II** in THF are *longer by a factor of 150−230* with respect to that observed for CuTPP in this solvent.[26a] In any event, while (porphinato)copper(II) species having an a_{1u} HOMO, such as (octaethylporphinato)copper(II) (CuOEP), typically have longer triplet lifetimes with respect to analogous species having an a_{2u} HOMO, such as CuTPP, it is interesting to note the lifetimes of CuOEP and CuTPP differ only by a factor of 4 in THF.[28a] While the origin of the enhanced lifetimes for **I** and **II** is unclear at present,[31] it is likely either (i) the energy gap between **I** and **II**'s triplet manifold and the (d, d) and CT quenching states that have been identified for CuTPP is larger than in this benchmark chromophore or (ii) different quenching states determine **I** and **II**'s lifetimes in THF. A possible origin for this behavior may derive from the π-conjugating *meso*-arylethynyl moieties, which likely affect the Lewis acidity of Cu^{2+}, potentially impacting the axial ligand affinity of these species in their ground and/or excited states. This hypothesis is consistent with the fact that **I** and **II**'s trip-multiplet lifetimes in benzene are long with respect to those observed in THF, suggesting the importance of a quenching state whose effect is more pronounced upon coordination of solvent.

Qualitative similarities in the transient absorption properties of our donor−acceptor complexes and of CuTPP allow us to use a single model to explain their excited state dynamics. Either a vibronic interaction or direct quenching by a short-lived excited state determines the relaxation time of the $^2T-{}^4T$ manifold. Coordination of a solvent molecule in either the ground or excited state enhances the relaxation. The observation that quenching of the $^2T-{}^4T$ manifold is less effective in our donor−acceptor complexes than in CuTPP may be a consequence of the substantial electronic coupling that exists between the porphyrin core and the *meso*-arylethynyl moieties. In order to determine how the electronic coupling between these groups in the triplet state compares with that observed for the ground state, we examined the time-resolved resonance Raman spectroscopy of these species.

Dynamics of Excited States Observed by Time-Resolved Resonance Raman Spectroscopy. Two-laser time-resolved resonance Raman spectroscopy on the nanosecond time scale probes the $^2T-{}^4T$ manifold of copper(II) porphyrins selectively.[25,28] Two distinct features are apparent in the time-resolved resonance Raman spectrum of compound **II** (Figure 8, inset). Namely, upon formation of the $^2T-{}^4T$ manifold (i) ν_4 does not shift (relative to the FT Raman spectrum of the ground state) and (ii) the nitro band upshifts by 6 cm^{-1} (relative to the FT Raman spectrum of the ground state). The behavior of ν_4 is consistent with a (π, π^*) state that mixes with a CT state (*vide infra*).[25] The upshift in the nitro band may result from the rotation of the nitrophenyl group out of the plane of the porphyrin upon formation of the triplet excited state. In any event, these data suggest that **II**'s triplet state possesses a similar degree of CT character relative to the ground state. Clearly, the resonance Raman data (Table 2, Figure 6) indicate that the initially prepared sing-doublet excited state features a substantial redistribution of electron density with respect to the ground state (Figure 5). Moreover, because the nitro group, for example, is much more strongly coupled in the initially prepared excited state, it suggests that this state exhibits substantial CT character. Because these data argue that electronic excitation into the B band at 441.6 nm should produce a state with different characteristics than were observed in both the time-resolved Raman and transient absorption experiments, we sought to probe states with lifetimes shorter than that of the $^2T-{}^4T$ manifold.

Dynamics of Excited States Observed by Transient Resonance Raman Spectroscopy. It has been shown that (porphinato)copper(II) excited states with short lifetimes, such as CT or (d, d) states, may be probed by one-laser, transient resonance Raman spectroscopy.[13,25,32] Our transient Raman strategy for compounds **I** and **II** is similar to that used by de Paula et al.[13] and Jeoung et al.[25] to study quenching states in CuTPP, which utilized a laser wavelength within the ground state Soret band and relatively far away from the absorption spectrum of the $^2T-{}^4T$ manifold. Given the long triplet lifetime and the fact that it absorbs weakly at 436 nm, due to the

(31) Enhanced triplet lifetimes of similar magnitude have been observed in other coordinating solvents. LeCours, S. M.; Phillips, C. M.; Therien, M. J. Unpublished results.

(32) Additional examples include the following: (a) Findsen, E. W.; Shelnutt, J. A.; Ondrias, M. R. *J. Phys. Chem.* **1988**, *92*, 307−314. (b) Crawford, B. A.; Ondrias, M. R. *J. Phys. Chem.* **1989**, *93*, 5055−5061. (c) Strahan, G. D.; Lu, D.; Tsuboi, M.; Nakamoto, K. *J. Phys. Chem.* **1992**, *96*, 6450−6457. (d) Jeoung, S. C.; Kim, D.; Cho, D. W., Yoon, M.; Ahn, K.-H. *J. Phys. Chem.* **1996**, *100*, 8867−8874.

Table 3. Raman Ground and Excited State Band Assignments for Compound **II**

	vibrational frequencies (cm^{-1})			
	ground state			excited state
mode description[a]	Fourier transform Raman	resonance Raman (441.6 nm)	resonance Raman (436 nm)	transient resonance Raman (436 nm)
ν_1	1238	1235	*f*	1227
NO_2	1337	1338	1335	1324
ν_4 ($C_\alpha N$, $C_\alpha C_\beta$)	1362	1359	1355	1348
ν_{20} ($C_\alpha C_{meso}$)	*b*	1538	*f*	1542
ν_2 ($C_\alpha C_{meso}$, $C_\beta C_\beta$)	1560	1568	1566	1571
($C_{PhB}C_{PhB}$)	(1605, 1596)[c]	(1611, 1599)[c]	*f*	(1607, 1598)[c]
ethyne	(2181, 2196)[d]	2194[e]	*f*	2192[e]

[a] Tentative assignments. Mode descriptors are taken from ref 19 unless otherwise indicated. The NO_2 and ethyne modes were assigned by reference to previously studied benchmark compounds (see ref 30). [b] Weak or not observed. [c] Two frequencies observed. The first value in parentheses corresponds to C−C stretching of the (dimethylamino)phenyl moiety and the second to the nitrophenyl moiety. [d] Two frequencies observed. The first value in parentheses corresponds to the ethyne directly linked to the (dimethylamino)phenyl moiety and the second to the nitrophenyl moiety. [e] Only the frequency of the ethyne directly linked to the nitrophenyl moiety is observed. [f] Assignment not made due to spectral congestion and/or large spectral shift.

substantial transient bleach observed at this wavelength (Figures 3 and 4), any states that absorb strongly at 436 nm and have lifetimes as short as 100 ps can be probed selectively in the transient Raman experiment.

Results from our electronic structure calculations provide a basis for interpretation of both time-resolved and transient Raman spectra. Given the similarities between the frontier orbitals of compounds **I** and **II** and those of D_{4h} porphyrins, we may use the arguments put forth by de Paula et al.[12,13] to predict shifts in the vibrational spectrum of the porphyrin moiety upon formation of (π, π^*) states. Considering compound **II**, for example, we observe (Figure 10) that in the HOMO − 1 (a_{2u} in D_{4h} symmetry) the $C_\alpha N$ interaction is slightly antibonding in character; in the LUMO and LUMO + 1, however, the $C_\alpha N$ interactions are clearly net antibonding. Hence, promotion from the HOMO − 1 to either the LUMO or LUMO + 2 results in weakening (downward frequency shifts) of the $C_\alpha N$ bonds. Because the $C_\beta C_\beta$ interaction is essentially nonbonding in character in the LUMO and LUMO + 1 while antibonding in the HOMO − 2, an excited state configuration involving these orbitals (analogous to the ($a_{1u}e_g$) configuration in D_{4h} symmetry) leads to strengthening of the $C_\beta C_\beta$ bonds. Similar arguments lead to the conclusion that the $C_\alpha C_\beta$ and $C_\alpha N$ bonds are correspondingly weakened. Figure 10 also suggests that modes composed of NO_2 stretches should shift to lower frequencies upon promotion of electrons from the HOMO − 1 or HOMO − 2 to either the empty LUMO or LUMO + 2; such excited configurations correspond to porphyrin-to-nitro CT states.

Because such CT states are predicted to exist for both compounds **I** and **II**, we must also consider the effect of partial oxidation and reduction of the porphyrin ring on their transient Raman spectra. Czernuszewicz et al.[20] have determined that cation radicals of copper(II) porphyrins with a_{2u} character, such as $CuTPP^+$, show downshifts in ν_4 and ν_2 relative to the neutral species. On the other hand, cation radicals with a_{1u} character, such as $CuOEP^+$, show downshifts in ν_4 and upshifts in ν_2 relative to the neutral species. Data for anion radicals of copper(II) porphyrins are not available, but Bocian and co-workers[19,33] have studied $ZnOEP^-$ and $ZnTPP^-$. They find that reduction of ZnTPP results in a small (4 cm^{-1}) downshift in ν_4 and in a splitting of ν_2 with one component upshifted by only 1 cm^{-1} and the other downshifted by 14 cm^{-1}. Reduction of ZnOEP does not shift ν_2 and downshifts ν_4 by 7 cm^{-1}.

In systems where both (π, π^*) and CT states are close in energy, such as CuOEP and CuTPP, the predictions for frequency shifts upon formation of (π, π^*) states must be amended. Jeoung et al.[25] have shown that the time-resolved Raman spectra of the $^2T-^4T$ states of CuOEP and CuTPP show very minor, or no, shifts in ν_4. This was seen as a result of mixing between (π, π^*) and CT states in the formation of the trip-multiplet states.

We now apply the principles described above to the transient Raman data obtained for electronically asymmetric compound **II** (Figure 8). The transient resonance Raman spectrum of compound **II** indicates that (i) ν_4 and the nitro band downshift 14 and 13 cm^{-1}, respectively, relative to the FT Raman spectrum of the ground state and (ii) ν_2 upshifts 11 cm^{-1} (relative to the FT Raman spectrum of the ground state). The behavior of ν_2, ν_4, and nitro bands is thus consistent with an electronically excited state that features a porphyrin core with cation radical character. Moreover, it suggests that this excited state species is formed by promotion of an electron from an a_{1u}-like orbital (HOMO − 2, a″ symmetry, Figure 10).

The vibrational properties of the state probed via the transient Raman experiment at 436 nm are distinctly different from those observed for the $^2T-^4T$ state. Our spectral assignments, summarized in Table 3, are as follows.

(i) Our electronic structure calculations predict that compound **II** should exhibit a slight decrease in bond order for both ethynyl moieties in the excited state with respect to the ground state (Figure 10). We do not observe this effect in the transient Raman spectra;[23] this may be due to power broadening effects that may mask minor spectral shifts occurring in the ethynyl region.

(ii) The bands at 1598 and 1607 cm^{-1} (Figure 8A) are probably C−C stretching modes of the phenyl groups in the (nitrophenyl)ethynyl and [(dimethylamino)phenyl]ethynyl moieties, respectively. The fact that these bands do not shift in frequency upon electronic excitation is consistent with our ZINDO calculations (Figure 10), which show that the HOMO − 2, HOMO − 1, and LUMO + 1 do not have significant electron density in these phenyl groups. Likewise, while the LUMO and LUMO + 2 do exhibit significant electron density on the (nitrophenyl)ethynyl moieties, the arene ring-localized orbitals are essentially nonbonding in character.

(iii) The band at 1571 cm^{-1} (Figure 8A), assigned as ν_2 ($C_\beta C_\beta$) of the excited state, upshifts by 11 cm^{-1} relative to the ground state spectrum obtained at 436 nm (Figure 5B). It is important to emphasize that in contrast, the ν_2 mode of CuTPP downshifts by 20 cm^{-1} in the LMCT excited state and by 3 cm^{-1} in the MLCT or (d, d) excited state.[13]

(iv) The broad band at 1542 cm^{-1} is consistent with the ν_{20}

(33) Perng, J.-H.; Bocian, D. F. *J. Phys. Chem.* **1992**, *96*, 4804−4811.

Table 4. Resonance Raman Vibrational Band Assignments for Compound **I**

	vibrational frequencies (cm^{-1})			
	ground state			excited state
mode description[a]	Fourier transform Raman	resonance Raman (441.6 nm)	resonance Raman (436 nm)	transient resonance Raman (436 nm)
ν_1	1234	1241	1247	1228
NO_2	1342	1343	1336	1323
ν_4 ($C_\alpha N$, $C_\alpha C_\beta$)	1364	1365	*c*	1347
$\nu_2 0$ ($C_\alpha C_{meso}$)	*b*	1537	*c*	1537
$\nu_2 0$ ($C_\alpha C_{meso}$)	*b*	*b*	*c*	1550
ν_2 ($C_\beta C_\beta$,$C_\alpha C_{meso}$,)	1560	1563	1566	1568
($C_{PhB}C_{PhB}$)	1595	1597	1598	1596
ethyne	2195	2195	*d*	2195

[a] Tentative assignments. Mode descriptors are taken from ref 19. The NO_2 and ethyne modes were assigned by reference to previously studied benchmark compounds (see ref 30). [b] Weak or not observed. [c] Not readily assignable due to spectral congestion or low intensity. [d] Experiment not performed.

($C_\alpha C_{meso}$) mode observed in CuTPP.[19] There may be more than one peak buried within this envelope.

(v) Two low-intensity bands appear at 1290 and 1450 cm^{-1} which are probably due to ν_{27} and ν_{28} in the excited state. Both of these modes were also observed in the transient resonance Raman spectrum of CuTPP in THF.[13]

(vi) The band at 1348 cm^{-1} is assigned as ν_4 ($C_\alpha N$) of the excited state and is downshifted by 7−14 cm^{-1} relative to the ground state spectrum, consistent with the expectation based on our electronic structure calculation. In CuTPP, the ν_4 mode downshifts by 24 cm^{-1} in the LMCT state and by 4 cm^{-1} in the MLCT or (d, d) state.[13]

(vii) The nitro band downshifts by 13 cm^{-1} upon formation of the excited state at 436 nm.

(viii) The band at 1227 cm^{-1} is probably ν_1 of the excited state and is downshifted by 11 cm^{-1} relative to the ground state spectrum.[34] The ν_1 mode of CuTPP also downshifts upon electronic excitation, albeit by only 3−4 cm^{-1}.[13]

We conclude that high-power pulsed excitation at 436 nm probes only one excited electronic state of compound **II**, whose vibrational spectrum differs from the spectrum of the ground state by an upshift of ν_2 and downshifts in ν_4 and nitro bands. Furthermore, the Raman spectroscopic signature of this state does not resemble that of the triplet state, which was probed in the time-resolved Raman experiment. The behavior of ν_2 and ν_4 is consistent with removal of electron density from a porphyrin-based molecular orbital with a″ symmetry (a_{1u} in the D_{4h} point group). The downshift in the nitro mode is consistent with occupancy of either empty a′ orbital. We also suggest that the filled a″ orbital is higher in energy in this state than the filled a′ orbital, in contrast to the results of our ZINDO calculations carried out for the ground state electronic structure (Figure 10).

Nearly all of the points raised above for compound **II** apply to the transient resonance Raman spectrum of compound **I** (Figures 7 and 8, Table 4). Namely, the upshift in ν_2 and downshifts in both ν_4 and the nitro mode are consistent with formation of a porphyrin-to-nitro CT state where electron density is removed from the a_u orbital (a_{1u} in D_{4h} symmetry).

(34) We considered two alternative assignments for the 1227 cm^{-1} band: ν_{22} ($C_\alpha N$) and ν_{31} ($C_\beta H$ in-plane deformation). While the ν_{22} mode would be expected to downshift, the ν_{31} mode would be expected to be relatively insensitive to photoexcitation. On the basis of this prediction, we suggest that the 1228 cm^{-1} band arises from either ν_1 or ν_{22}. However, whether the band is due to ν_1 or ν_{22} does not influence significantly our analysis of the transient Raman spectrum of compound **I**.

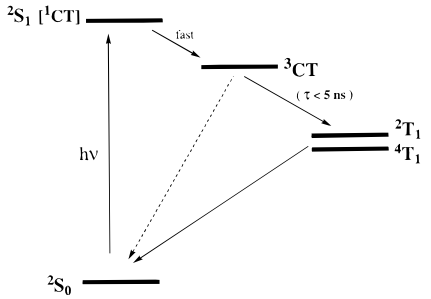

Figure 11. Summary of the proposed excited state dynamics for compounds **I** and **II**.

The main difference in the vibrational properties of the excited state probed in the transient Raman experiment between compounds **I** and **II** lies in the behavior of the nitro band. While the nitro band for compound **II** is located at 1337 cm^{-1} in the FT Raman spectra, the analogous nitro stretching frequency for compound **I** is located at 1342 cm^{-1}. Compound **II**'s 1337 cm^{-1} band lies 11 cm^{-1} to lower frequency with respect to the analogous band in (4-nitrophenyl)acetylene. Because the location for the nitro band in the excited state is similar for both compounds (approximately 1323 cm^{-1}; see Figures 7A and 8A), we suggest that more porphyrin-to-nitro CT character is mixed into the ground state for compound **II**, consistent with the expectation that the electron-releasing [(dimethylamino)phenyl]-ethynyl moiety should make **II**'s porphyrin macrocycle more electron rich than **I**'s (Figures 9 and 10). Furthermore, while both compounds **I** and **II** show N−O antibonding character (data not shown) in the HOMO − 1, Mulliken population analysis of this orbital shows that **II** has more N- and O-atom-centered electron density in this orbital with respect to **I**, congruent with the FT Raman data. Finally, since the shifts of all bands in the excited state with respect to the ground state are similar for both compounds, this signifies that the extent of charge delocalization from the porphyrin to the nitro substituent must be similar for both **I** and **II**.

Conclusions

A model for the excited state dynamics of compounds **I** and **II** is presented in Figure 11, which is based upon the results obtained from the FT, resonance, time-resolved resonance, and transient resonance Raman spectroscopic experiments, as well as the data obtained from our transient absorption studies. The resonance and FT Raman data suggest that excitation into the Soret band produces an excited state, denoted as $^2S_1$ (^{1}CT) in Figure 11, that has enhanced charge-transfer character with respect to the ground state ($^2S_0$). The transient absorption experiments and time-resolved Raman data evince that the triplet manifolds of compounds **I** and **II** bear many features in common with the ^{2}T−^{4}T states of CuTPP; most importantly, neither experiment suggests that the long-lived triplet states of **I** and **II** have significant CT interactions involving the porphyrin and the pendant arylethynyl groups. Because the initially prepared excited state ($^2S_1$) has augmented porphyrin-to-(nitrophenyl)-ethynyl CT character with respect to that observed for $^2S_0$, we argue that the state we probe in the transient resonance Raman experiment is best formulated as a ^{3}CT state, since it bears so many vibrational signatures in common with that which would be expected for $^2S_1$, on the basis of our electronic structure calculations. Congruent with the short (τ < 350 fs) lifetime of $^2S_1$ for CuTPP, we propose that $^2S_1$ for compounds **I** and **II** rapidly decays, but in our case, to a ^{3}CT state. The ^{3}CT state, though probed via transient Raman methods, must be relatively short-lived as well (τ < 5 ns) because no evidence for this state

is present in the transient absorption and time-resolved Raman experiments.

Studies of [5,15-bis[(4′-nitrophenyl)ethynyl]-10,20-diphenylporphinato]copper(II) and [5-[[4′-(dimethylamino)phenyl]ethynyl]-15-[(4″-nitrophenyl)ethynyl]-10,20-diphenylporphinato]-copper(II) suggest important ways to tune the photophysical properties of copper(II) porphyrins. At least in compound **II**, production of the electronically excited CT state leads to a substantial change in the dipole moment of the molecule. We conclude that compounds **I** and **II** are important members of a new class of chromophores that can undergo long-range, fast, charge migration upon electronic excitation. Given the polarizable nature of the porphyrinic core, the large oscillator strength of porphyrin-centered transitions, and the fact that these charge-transfer states may be formed very efficiently with pulsed laser excitation, molecules based on this structural motif represent a new direction in the design of chromophores relevant to optoelectronic devices and materials.[16]

Acknowledgment. J.d.P. gratefully acknowledges funding from the Kresge Foundation and the National Science Foundation (Grant CHE-9530707). M.J.T. is indebted to the National Institutes of Health (Grant GM 48130-01A1.4) and the Office of Naval Research (Grant 96-1-0725) for their research support, and to the Searle Scholars Program (Chicago Community Trust), the Arnold and Mabel Beckman Foundation, E. I. du Pont de Nemours, and the National Science Foundation for Young Investigator Awards, as well as to the Alfred P. Sloan and Camille and Henry Dreyfus Foundations for research fellowships. Transient triplet−triplet absorption spectra were obtained at the NIH-supported Regional Laser and Biotechnology Laboratory (RLBL) located at the University of Pennsylvania. The authors thank Dr. Ranjit Kumble, Professor Valerie A. Walters, and Mr. John Vrettos for helpful discussions.

Supporting Information Available: Transient resonance Raman spectra of the ethynyl region of compounds **I** and **II** in THF obtained with pulsed excitation at 436 nm (6 pages). See any current masthead page for ordering and Internet access instructions.

JA964436J